

## Eureka Journal of Geoscience, Materials & Resource Engineering (EJGMRE)

ISSN 2760-4985 (Online) Volume 02, Issue 06, June 2026



This article/work is licensed under CC by 4.0 Attribution

<https://eurekaoa.com/index.php/9>

# NATURE-BASED SOLUTIONS FOR URBAN FLOODING AND WATER REUSE IN IRAQI CITIES: EVALUATING GREEN INFRASTRUCTURE UNDER CLIMATE STRESS

Rusul A Al-ameri

Al-Furat Al-Awsat Technical University, Najaf Technical Institute

rusulalameri93@gmail.com

### Abstract

Urban flooding is increasingly affecting semi-arid cities where rapid urbanisation, high impervious surface coverage, and climate-driven extreme rainfall events exceed the capacity of conventional drainage systems. Existing studies often evaluate flood hazards or infrastructure upgrades independently, without integrating hydrodynamic modelling, spatial optimisation, climate stress simulation, and stormwater reuse potential within a unified framework. To address this limitation, an integrated SWMM–GIS–NbS framework for urban flood resilience is developed to evaluate the effectiveness of nature-based solutions (NbS) in reducing run-off, improving drainage performance, and supporting stormwater reuse under climate stress conditions in Iraqi cities. The framework combines EPA SWMM hydrodynamic simulation, GIS-based spatial analysis, and green infrastructure scenario modelling using geospatial datasets, including USGS EarthExplorer SRTM Digital Elevation Model (DEM), NASA POWER precipitation records, and the Zenodo global land cover dataset. Terrain analysis, rainfall processing, and impervious surface estimation are integrated to simulate flood behaviour and optimise the placement of green infrastructure such as permeable pavements, bioswales, and green roofs. Simulation results demonstrate that the proposed framework significantly improves flood mitigation

## Eureka Journal of Geoscience, Materials & Resource Engineering (EJGMRE)

ISSN 2760-4985 (Online) Volume 02, Issue 06, June 2026



This article/work is licensed under CC by 4.0 Attribution

<https://eurekaoa.com/index.php/9>

performance, reducing peak run-off to 16.75 m<sup>3</sup>/s, decreasing flooded nodes to 18, achieving 31.7% run-off reduction, and increasing infrastructure efficiency to 76.5% under climate-intensified rainfall scenarios. Additionally, stormwater harvesting from green infrastructure contributes 38.9% reuse potential and enhances climate resilience by 67.8%. The proposed framework provides a scalable decision-support approach for climate-adaptive urban water management in semi-arid regions.

**Keywords:** Nature-Based Solutions, Urban Flood Resilience, Green Infrastructure, Climate Stress Hydrology, SWMM–GIS–NbS Modelling.

### 1. Introduction

The world population is expanding rapidly; this is due to the increasing population, growth in the economy, and spatial development of the city setting (Mustafa et al., 2025). With the growth of cities, natural landscapes are increasingly being covered with buildings, transport systems, and other impervious surfaces that alter significantly the hydrological processes in the urban areas (Patel et al., 2024). This process interrupts the natural infiltration routes, increases surface run-offs, and decreases the recharge ability of the groundwater (Kumar et al., 2023). The problem of urban flooding has therefore become a major environmental and infrastructural issue that is experienced in cities in different climatic conditions (Kaiser & Akter, 2025). Even those regions that are traditionally defined by average quantities of precipitation that are relatively low per year are starting to experience events of short-lived, increase in intensity rainfall that may outperform the design capacity of the conventional drainage systems (Reulen et al., 2024). The occurrence of flood-induced disruptions has been on the rise in terms of frequency and severity over the past decades, based on two drivers that have interacted with each other, namely, rapid urbanisation and climate variability (Aljaff, 2025, pp. 1118–1128). Increasing



## Eureka Journal of Geoscience, Materials & Resource Engineering (EJGMRE)

ISSN 2760-4985 (Online) Volume 02, Issue 06, June 2026



This article/work is licensed under CC by 4.0 Attribution

<https://eurekaoa.com/index.php/9>

urban areas consolidate people, infrastructure, and economic activity in small space areas, increasing the exposure to hydrological extremes (Savelli et al., 2026).

Meanwhile, the alterations in rain patterns (especially the increase of the extreme precipitation cases) introduce further burden to stormwater management systems that were initially developed based on the historical climate conditions. The classical drainage systems prioritises on swift run-off movement by underground pipes and channels, which is about efficient water removal instead of distributed storage and infiltration (Douabul, 2025). Although these systems may accommodate moderate rainfall, in most cases, they fail to be flexible in the changing climatic conditions, and thus, they lead to greater surface flooding during severe storms (Hassan et al., 2023). To address these challenges, the scope of urban water management has been progressively shifting to adopt more comprehensive and sustainable solutions to the problems instead of the strictly structural engineering-based methods. In this paradigm shift, nature-based solutions (NbS) and green infrastructure (GI) have been of significant academic and policy attention and city policy strategies (Al-Hagla & Alrawaf, 2025). GI incorporates the natural hydrology of the infiltration, evapotranspiration, and temporary surface storage in the urban area instead of using grey infrastructure only (Kemal et al., 2025). The prevalent GI features are permeable pavements, green roofs, rain gardens, bio-swales, and built wetlands. These systems decrease the stormwater run-offs and at the same time produce numerous environmental amenities such as regulation of the microclimate of urban areas, creation of biodiversity, air quality, and aesthetic worth of urban landscapes.

Another benefit of green infrastructure is its ability to accommodate stormwater harvesting and reuse (Mutar & Abdullah, 2025, pp. 3045–3055). Stormwater collected with distributed GI systems can be collected and used in water-scarce areas to irrigate the land, do landscaping, and other non-potable purposes. This is dual-functional: flood control and water resource enhancement make GI a

## Eureka Journal of Geoscience, Materials & Resource Engineering (EJGMRE)

ISSN 2760-4985 (Online) Volume 02, Issue 06, June 2026



This article/work is licensed under CC by 4.0 Attribution

<https://eurekaoa.com/index.php/9>

strategic element of sustainable urbanization (AL-Hudaib et al., 2025). Although there is emerging evidence across the world in support of the GI implementation, distinct contextual disparities between temperate and arid environments in terms of urban areas are also significant (Gao et al., 2024, pp. 679–694). The semi-arid cities usually have low annual rainfall but severe episodic storms that produce a high rate of water run-off on the highly impervious surfaces (Allafta et al., 2026). Also, infrastructure ageing, sedimentation, and unplanned urban growth may limit drainage performance (Ebraheem et al., 2024, pp. 4715–4726). The following conditions demonstrate the need for region-specific evaluation with the use of combined hydrological modelling, geographic information systems, and climate scenario analysis to assess the efficiency of the nature-based flood mitigation measures in the context of changing environmental pressures (Olgun et al., 2024).

### 1.2 Research Motivation

Nevertheless, despite the substantial body of literature that underscores the environmental and socio-ecological advantages of green infrastructure, most of the studies are conceptual or geographically inclined towards the temperate regions. In dry and semi-arid urban environments in developing situations, there are no integrated quantitative tests of hydrological simulation, climate stress conditions, spatial optimisation, and stormwater reuse appraisal. The available studies often look at isolated flood hazard dimensions devoid of mitigation performance evaluation, or analyse the efficiency of infrastructure without considering the forecasted climate variability. Such disciplinary fragmentation limits evidence-based urban water management decisions. The current study is driven by the fact that integrated modelling frameworks are necessary to examine the effectiveness of flood reduction and the potential of stormwater reuse at the same time under future climate conditions through the GIS-based hydrological simulation techniques.

## Eureka Journal of Geoscience, Materials & Resource Engineering (EJGMRE)

ISSN 2760-4985 (Online) Volume 02, Issue 06, June 2026



This article/work is licensed under CC by 4.0 Attribution

<https://eurekaoa.com/index.php/9>

### 1.3 Problem Statement

The concept of floods in urban areas that are semi-arid cities is a hydrological anomaly. Although the amount of rainfall per year is characteristically low, intense short-duration convective storms often overtake urban drainage facilities, resulting in rapid surface run-off and occasionally causing floods. The traditional grey drainage systems, usually developed based on the rainfall statistics of the past, are insufficiently adaptive to the changing variability in precipitation brought about by climatic changes (Al-Bazaz, 2026). Even though nature based solution and green infrastructure have been extensively suggested as a sustainable approach in mitigating climate stress, the quantitative characteristics of them in real and expected climatic stressor conditions in most developing urban areas have not been adequately assessed. In addition, there is limited peer-reviewed evidence that combines hydrodynamic flood modelling and space optimization in the positioning of infrastructure (Tahir et al., 2026). As a result, the urban planners are not provided with empirical data on the effectiveness of individual GI designs to minimize run-off, mitigate peak discharge, and assist with stormwater reuse.

### 1.4 Objectives of the Study

The main aim of this research is to analyze the effectiveness of the nature-based solutions in terms of de-risking urban floods and increasing the potential stormwater reuse in an Iraqi urban city in a climate-stress environment. In particular, the research will have the following objectives:

- Model urban run-off and flood dynamics under present and projected climate scenarios.
- Assess the performance of multiple green infrastructure implementation scenarios.
- Quantify reductions in run-off volume, peak discharge, and flooded area.
- Optimise spatial prioritisation of GI using GIS-based multi-criteria analysis.

## Eureka Journal of Geoscience, Materials & Resource Engineering (EJGMRE)

ISSN 2760-4985 (Online) Volume 02, Issue 06, June 2026



This article/work is licensed under CC by 4.0 Attribution

<https://eurekaoa.com/index.php/9>

- Estimate the potential for harvested stormwater to contribute to urban water supply resilience.

The study, based on this integrated water resources engineering framework, will offer quantitative data that can be used to inform climate-adaptive urban planning approaches and upwardly sustainable flood management approaches in Iraq.

### 2. Related Works

Chairat and Gheewala (2024) proposed a quantitative framework of measuring Nature-based Solutions based on the combination of SEEA EA, LCA, Social LCA, and CBA according to the IUCN standards. The model made the NbS assessment standardized in terms of environment, social, and economic aspects. Nevertheless, it was still a conceptual framework with no hydrodynamic simulations or climate analysis, and could only be used to model floods in dry cities. Rodriguez et al. (2024) examined the resilience of green infrastructure on the combined sewer system based on Global Resilience Analysis and EURO-CORDEX climate projections (2085-2099). The findings indicated that the rainfall can enhance the overflow volumes by 145-256, and GI enhanced the resilience by 7-22. But the research focused exclusively on temperate sewerage as opposed to arid city settings. Ali and Mawlood (2023) simulated urban flooding in Erbil in SWMM by using rainfall data of 1992-2022 and hyetographs in IDF format. The infrastructure improvements have cut down the flooded nodes to 25 out of 33 during the 100-year storms. Though the research confirmed hydraulic performance, it did not include Nature-based Solutions and climate change conditions but rather concentrated on grey infrastructure.

The study by Tejero-Beteta et al. (2024) constructs a GIS-based optimisation model by assessing demand-responsive transport services based on a vehicle routing problem perspective. Operational efficiency and service coverage were evaluated in scenario simulations. The findings indicated that low-capacity vehicles were found to be more efficient in scattered areas. Nevertheless, the

## Eureka Journal of Geoscience, Materials & Resource Engineering (EJGMRE)

ISSN 2760-4985 (Online) Volume 02, Issue 06, June 2026



This article/work is licensed under CC by 4.0 Attribution

<https://eurekaoa.com/index.php/9>

study was on transportation mechanisms and not on flood resilience and hydrological modelling. Shaibu et al. (2025, pp. 122–135) tested sustainable urban water management measures incorporating the use of reuse, recycling, and technologies to mitigate climate risks that include built wetlands and membrane bioreactors. The research focused on new water security solutions but did not have hydrological data or flood modelling. It was therefore not practical and did not have space-based priority and quantitative flood reduction evaluation. Using rainfall records and the SCS-CN run-off model, Mustafa et al. (2025) compared the effects of impervious surface growth and rainwater harvesting on the flood resistance of Erbil. Findings revealed an almost dual run-off in impervious areas. Even though it applied to semi-arid Iraq, the study used a simplified estimation of run-off without SWMM simulation and climate projections. The available literature demonstrates the developments of NbS assessment, green infrastructure resilience, and flood modelling. Nonetheless, studies are still scattered together, without the incorporation of hydrodynamic modeling, climate modeling, GIS optimization, and evaluation of water reuse. This paper will fill such gaps by integrating SWMM simulation, climatic analysis, GIS-based prioritisation, and stormwater reuse estimation in Iraqi cities.

### 3. Materials and Methods

#### 3.1 Study Area

The study is carried out in the Republic of Iraq, which is in Western Asia between about 29°-37° N latitude and 38°-48° E longitude (Al Saady, 2023, pp. 158-183). The nation stands in the north-eastern part of the Arabian Plate and encompasses varied physiographic areas of the Mesopotamian alluvial plain, desert plateaus, and highlands of the north. The large cities such as Baghdad, Basra, and Karbala lie on the flat alluvial plains that are made up of the rivers Tigris and Euphrates. The climate is arid to semi-arid with hot and dry weather in summer and mild weather in the winter season. The rainfall is mostly experienced between

## Eureka Journal of Geoscience, Materials & Resource Engineering (EJGMRE)

ISSN 2760-4985 (Online) Volume 02, Issue 06, June 2026



This article/work is licensed under CC by 4.0 Attribution

<https://eurekaoa.com/index.php/9>

November and March, with an average amount of precipitation reaching below 100 mm in the south deserts and more than 400 mm in mountainous regions in the north (Awadh, 2023). Rapid urbanisation, rising impervious areas, and the deterioration of the drainage systems are some of the causes of episodic urban flooding due to short-duration extreme rainfalls.

### 3.2 Data Collection and Materials

The study used three official geospatial and meteorological data sets: the USGS EarthExplorer SRTM Digital Elevation Model (DEM), NASA POWER meteorological data, and the Copernicus Global Land Cover dataset. Such datasets give topographic, climatic, and land surface variables that are required in the hydrological modelling.

#### 3.2.1 Digital Elevation Model

The USGS Earth Explorer (U.S. Geological Survey, 2015) portal provided topographic data. The Shuttle Radar Topography Mission (SRTM) 1 Arc-Second Global DEM offers the values of the elevation in metres above the mean sea level with a spatial resolution of around 30 m in GeoTIFF format. Surface elevation is the main variable that is in the dataset. Slope, aspect, flow direction, and flow accumulation are some of the secondary terrain derivatives that can be produced using this elevation grid in GIS environments. These variables were applied to outline sub-catchments, demarcate drainage routes, and build up the topographic structure to be used in SWMM modelling.

#### 3.2.2 Rainfall Data

NASA Prediction of Worldwide Energy Resources (POWER) Data (National Oceanic and Atmospheric Administration, 2023). Access Viewer was used to get Meteorological data. The platform offers such satellite-derived variables as precipitation (PRECTOTCORR), near-surface air temperature (T2M), relative

## Eureka Journal of Geoscience, Materials & Resource Engineering (EJGMRE)

ISSN 2760-4985 (Online) Volume 02, Issue 06, June 2026



This article/work is licensed under CC by 4.0 Attribution

<https://eurekaoa.com/index.php/9>

humidity (RH2M), wind speed (WS2M), solar radiation (ALLSKY\_SFC\_SW\_DWN), and atmospheric pressure. In this research, the variable that was used was the PRECTOTCORR, which is bias-corrected daily precipitation in millimetres. The data can be extracted on hourly, daily, monthly, and climatological time scales. The rainfall inputs to simulate the run-off were obtained using the daily precipitation time-series data.

### 3.2.3 Land Use/Land Cover

The Copernicus global land service land cover 100m collection 3 (Epoch 2019) (Buchhorn et al., 2020) provided land cover data. The dataset is a discrete land cover classification in 23 classes that are based on the UN-FAO Land Cover Classification System. The major classes are urban/built-up areas, croplands, forests, grasslands, shrublands, bare areas, and water bodies. The first one is categorical land cover per 100 m resolution. The impervious surface distribution and run-off parameters in the hydrological model were obtained using these classifications.

### 3.3 Integrated SWMM–GIS–NbS Framework for Urban Flood Resilience

The methodology embraced in this study incorporates hydro modeling, geographical terrain processing, rain processing using climate conditions, and quantification of impervious surfaces into a systematic preprocessing and modeling procedure. Raw Digital Elevation Model (DEM), daily precipitation, and land use/land cover data were systematically prepared and then incorporated into the EPA Storm Water Management Model (SWMM). The terrain and slope derivation allowed the correct sub-catchment outlining and the routing of the flows. Rainfall filtering was done statistically to have a reliable design storm construction at baseline and stress conditions. Run-off parameter was assigned based on the reclassification of land cover by estimating the imperviousness. The processed data sets were then applied to SWMM to perform a simulation of run-

## Eureka Journal of Geoscience, Materials & Resource Engineering (EJGMRE)

ISSN 2760-4985 (Online) Volume 02, Issue 06, June 2026



This article/work is licensed under CC by 4.0 Attribution

<https://eurekaopenaccess.com/index.php/9>

off volume, peak discharge, and flood-prone nodes in various infrastructure conditions. This combined methodology will ensure physical consistency between the spatial inputs and hydraulic modelling to enhance the predictability of such a process in the semi-arid urban context, and also maintain methodological transferability to similar climate-related cities.

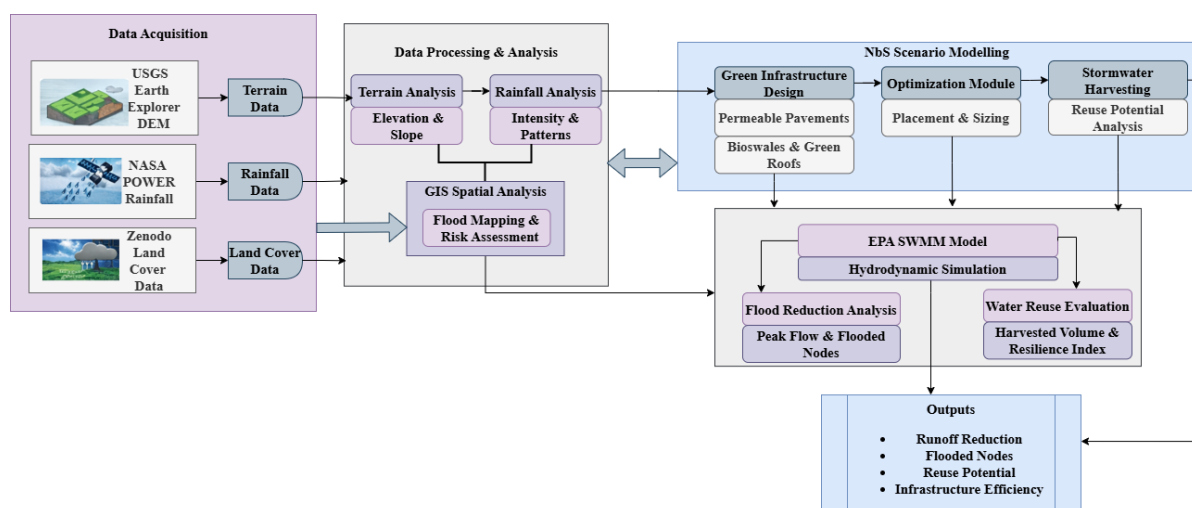


Fig. 1 Integrated SWMM–GIS–NbS Urban Flood Resilience Framework Architecture

Fig. 1 introduces a modelling framework of an integrated SWMM-GIS-NbS of urban flood resilience. There is terrain, rainfall, and spatial analysis of DEM, rainfall, and land cover data. The SWMM hydrodynamic simulations are guided by green infrastructure scenarios and optimisation to assess flood and run-off behaviours, as well as stormwater harvesting opportunities to manage urban water-related problems in climate-resilient urban water management.

### 3.3.1 Data Preprocessing

Raw DEM, rainfall, and land cover data were processed to be hydrologically consistent and compatible with SWMM. DEM voids were fixed, and terrain

## Eureka Journal of Geoscience, Materials & Resource Engineering (EJGMRE)

ISSN 2760-4985 (Online) Volume 02, Issue 06, June 2026



This article/work is licensed under CC by 4.0 Attribution

<https://eurekaoa.com/index.php/9>

derivatives were created, rainfall records were statistically cleaned and formatted, and the land cover was reclassified to generate impervious estimates that produced physically consistent parameters that could be used in flood simulation and green infrastructure analysis.

### a) DEM Void Filling and Terrain Derivation

DEM preprocessing was to eliminate sinks and void pixels, which disrupt the natural drainage flow. An algorithm to fill in depressions ensured hydrological integrity by resolving artificial depressions. Subsequently, a calculation of terrain slope gradients using elevation derivatives was used to depict the flow velocity, and this could be used to form a watershed and create sub-catchments in SWMM. The following equation (1) is the calculation of terrain slope magnitude:

$$S = \sqrt{\left(\frac{\partial z}{\partial x}\right)^2 + \left(\frac{\partial z}{\partial y}\right)^2} \times 100 \quad (1)$$

Where  $S$  is the slope percentage,  $\frac{\partial z}{\partial x}$  and  $\frac{\partial z}{\partial y}$  represent elevation gradients in the horizontal  $x$  and  $y$  directions derived from adjacent raster cells, and the multiplier converts the gradient to percentage form. The DEM was then corrected, and the slope grids were derived and used to delineate the watershed boundaries and produce the SWMM sub-catchment geometries.

### b) Rainfall Cleaning and Extreme Event Standardisation

Records of rainfall derived through satellites were filtered out for missing data, deviations, and unrealistic spikes. Z-score standardisation revealed the deviations of long-term averages, which guaranteed the statistical stability. Percentile thresholds were then used to define extreme rainfall events, and the corrected precipitation series was formatted into run-off simulation SWMM time-series

## Eureka Journal of Geoscience, Materials & Resource Engineering (EJGMRE)

ISSN 2760-4985 (Online) Volume 02, Issue 06, June 2026



This article/work is licensed under CC by 4.0 Attribution

<https://eurekaoa.com/index.php/9>

inputs. The index of filtering is the precipitation anomaly index (represented by the following (2):

$$Z_i = \frac{P_i - \bar{P}}{\sigma_P} \quad (2)$$

Where,  $Z_i$  is the standardised precipitation score for day  $i$ ,  $P_i$  is observed daily rainfall (mm),  $\bar{P}$  is the long-term mean daily rainfall, and  $\sigma_P$  is the standard deviation of the precipitation series. Days exceeding  $\pm 3$  standard deviations were inspected and corrected. The filtered rainfall record was converted to the form of run-off simulation time-series input files readable by SWMM.

### c) Land Cover Reclassification and Imperviousness Estimation

Land cover data was reclassified into hydrologically significant categories, and this is the type that was compatible with SWMM modelling. The impervious coefficients were used to classify built-up areas; the vegetation was considered low, and water bodies were not considered. The aggregation of the area was to represent the spatial variability of the urban surfaces by calculating the imperviousness of each of the sub-catchments. The impervious fraction of the sub-catchment is calculated as the following (3):

$$I_{sc} = \frac{\sum_{k=1}^n (A_k \times f_k)}{A_{total}} \times 100 \quad (3)$$

Where,  $I_{sc}$  represents the impervious percentage of sub-catchment  $sc$ ,  $A_k$  is the area of land cover class  $k$ ,  $f_k$  is the assigned impervious coefficient for class  $k$ , and  $A_{total}$  is the total sub-catchment area. This parameter of imperviousness directly controls the run-off production and infiltration processes of the SWMM model.

### 3.3.2 Integrated Hydro-Climatic GIS–SWMM Modelling Architecture

The model structure combines the spatial terrain processing, rainfall forcing generation, hydrological simulation, climate stress scaling, the allocation of green

## Eureka Journal of Geoscience, Materials & Resource Engineering (EJGMRE)

ISSN 2760-4985 (Online) Volume 02, Issue 06, June 2026



This article/work is licensed under CC by 4.0 Attribution

<https://eurekaoa.com/index.php/9>

infrastructure (GI), optimisation, and water reuse evaluation into a sequential computational framework. The spatial-hydrological input layer is made up of preprocessed DEM, rainfall, and land cover data. These factors are modelled in EPA SWMM 5.2 in order to model the dynamic rainfall-runoff routing on a climate-adjusted and a baseline scenario. GI elements are simulated as Low Impact Development (LID) controls with intensities of spatial coverage. The hydrological metrics of reduction and optimisation algorithms are used to measure performance outputs. The structure will guarantee physical uniformity, spatial expressiveness, and climate sensitivity applicable to semi-arid urban systems.

### a) Flood and Run-off Modelling

The flood procedures are modeled as EPA SWMM 5.2, where mass conservation and dynamic wave routing are implemented to model urban drainage systems. The excess of rainfall infiltration is what controls the process of surface run-off generation in each sub-catchment, and hydraulic routing takes into consideration conduit flow, storage nodes, and surcharge conditions. The following (4) represents the Green-Ampt formulation of infiltration:

$$f(t) = K_s \left( 1 + \frac{\psi \Delta \theta}{F(t)} \right) \quad (4)$$

Where,  $f(t)$  is infiltration rate (mm/hr),  $K_s$  saturated hydraulic conductivity (mm/hr),  $\psi \Delta \theta$  capillary suction head (mm),  $\Delta \theta$  soil moisture deficit, and  $F(t)$  cumulative infiltration depth (mm). The continuity relationship of surface run-off is given as follows (5):

$$\frac{dV}{dt} = I(t) - Q(t) - f(t) \quad (5)$$

Where  $V$  is surface storage volume ( $\text{m}^3$ ),  $I(t)$  rainfall intensity input,  $Q(t)$  run-off discharge, and  $f(t)$  infiltration loss. The following (6) is the dynamic wave momentum routing in conduits:

## Eureka Journal of Geoscience, Materials & Resource Engineering (EJGMRE)

ISSN 2760-4985 (Online) Volume 02, Issue 06, June 2026



This article/work is licensed under CC by 4.0 Attribution

<https://eurekaopenaccess.com/index.php/9>

$$\frac{\partial Q}{\partial t} + gA \frac{\partial H}{\partial x} + gAQ|Q|/(C^2R) = 0 \quad (6)$$

Where  $Q$  is discharge,  $g$  is gravitational acceleration,  $A$  is flow area,  $H$  is hydraulic head,  $C$  is Manning roughness coefficient term, and  $R$  is hydraulic radius. These equations can be used to physically simulate the flood propagation process in different rainfall intensities.

### b) Climate Stress Scenarios

Climate stress scenarios are created through varying the intensity of baseline precipitation to represent the projected increases in extreme rainfall in the region. NASA POWER rainfall has been observed (2000-2023) as a baseline reference distribution. Scaling factors formulated based on SSP2-4.5 and SSP5-8.5 projections produce moderate and extreme future scenarios. The following (7) is the scaling transformation of the rainfall:

$$P_{future} = P_{observed}(1 + \delta) \quad (7)$$

Where,  $P_{future}$  is adjusted rainfall depth (mm),  $P_{observed}$  baseline extreme rainfall, and  $\delta$  climate scaling factor (0.15 or 0.30). The forecasted difference at the index of rainfall intensity is calculated as (8):

$$I_{cc} = \frac{P_{future} - P_{observed}}{P_{observed}} \times 100 \quad (8)$$

Where,  $I_{cc}$  is the percentage intensity change. The following (8) formulates the design storm depth-duration adjustment:

$$D_{adj} = D_{base}(1 + \delta)^\beta \quad (9)$$

Where,  $D_{adj}$  adjusted storm duration depth,  $\beta$  empirical intensity-duration exponent. These scaled rain series do produce synthetic storm hyetographs to be used in SWMM simulations under climatic stress.

## Eureka Journal of Geoscience, Materials & Resource Engineering (EJGMRE)

ISSN 2760-4985 (Online) Volume 02, Issue 06, June 2026



This article/work is licensed under CC by 4.0 Attribution

<https://eurekaoa.com/index.php/9>

### c) Green Infrastructure (GI) Scenarios

Three GI conditions are the simulation of Low Impact Development (LID) deployment of different intensities across sub-catchments. GI elements consist of permeable pavements, bioswales, buildings, and constructed wetlands. In SWMM, all elements are discussed as storage-infiltration units, which alter the generation of the surface run-off. The following (10) represents the LID area fraction:

$$F_{LID} = \frac{A_{LID}}{A_{sc}} \times 100 \quad (10)$$

Where,  $F_{LID}$  is the percentage GI coverage,  $A_{LID}$  GI area, and  $A_{sc}$  sub-catchment area. The reduction of effective imperviousness as a result of GI is computed as (11) follows:

$$I_{eff} = I_{base} \left(1 - \frac{F_{LID}}{100}\right) \quad (11)$$

Where,  $I_{eff}$  is the modified impervious fraction. The following (12) defines the GI storage capacity per sub-catchment:

$$S_{GI} = A_{LID} \times d_{storage} \quad (12)$$

Where,  $S_{GI}$  is the total GI storage volume ( $m^3$ ) and  $d_{storage}$  design storage depth (m). Such relations change run-off response depending on different GI implementation degrees.

### d) Performance Evaluation

The evaluation of model outputs is done through run-of-river reduction, discharge attenuation, and flooding evaluations. Comparison is made between the situation at baseline and GI at both climate conditions. The indicator of run-off volume reduction looks as follows (13):

$$RVR = \frac{V_{baseline} - V_{GI}}{V_{baseline}} \times 100 \quad (13)$$

Where,  $V_{baseline} - V_{GI}$  represent run-off volumes ( $m^3$ ). The highest discharge cut-off measure is characterized by the following (14):

## Eureka Journal of Geoscience, Materials & Resource Engineering (EJGMRE)

ISSN 2760-4985 (Online) Volume 02, Issue 06, June 2026



This article/work is licensed under CC by 4.0 Attribution

<https://eurekaoa.com/index.php/9>

$$PDR = \frac{Q_{baseline} - Q_{GI}}{Q_{baseline}} \times 100 \quad (14)$$

Where,  $Q_{baseline}$  and  $Q_{GI}$  are maximum discharge rates ( $m^3/s$ ). The reduction ratio of flood nodes is developed by the following (15):

$$FNR = \frac{N_{baseline} - N_{GI}}{N_{baseline}} \times 100 \quad (15)$$

Where  $N$  denotes the number of surcharged nodes, these measures are used to measure hydrologic or hydraulic enhancements that have been realized by GI interventions.

### e) Optimisation of GI Placement

Spatial optimisation uses the Multi- Criteria Decision Analysis (MCDA) that is based on GIS and embedded with Analytic Hierarchy Process (AHP). These criteria are slope, imperviousness, zonation of rainfall, and proximity to drainage. The following (16) represents the AHP consistency ratio:

$$CR = \frac{CI}{RI} \quad (16)$$

Where,  $CI = (\lambda_{max} - n)/(n - 1)$ ,  $n$  criteria number, and  $RI$  random index. The index of weighted suitability is calculated by the following (17):

$$SI = \sum_{i=1}^n w_i x_i \quad (17)$$

Where,  $w_i$  is weight and  $x_i$  normalised criterion score. Normalisation procedure is written as follows (18):

$$x_i = \frac{X_i - X_{min}}{X_{max} - X_{min}} \quad (18)$$

Where,  $X_i$  raw value and  $X_{max} - X_{min}$  range limits. High SI values are priority GI deployment zones.

### f) Water Reuse Potential Assessment

GI systems offer the storage capacity of stormwater harvesting. SWMM storage outputs and estimates of irrigation demand are used to quantify the potential of

## Eureka Journal of Geoscience, Materials & Resource Engineering (EJGMRE)

ISSN 2760-4985 (Online) Volume 02, Issue 06, June 2026



This article/work is licensed under CC by 4.0 Attribution

<https://eurekaoa.com/index.php/9>

the annual reuse. The following (19) represents the ratio of water reuse contribution:

$$WRC = \frac{SV \times \eta}{D_{irr}} \times 100 \quad (19)$$

Where,  $SV$  stored volume ( $m^3/year$ ),  $\eta$  efficiency factor, and  $D_{irr}$  irrigation demand. The summation of the annual stored volume is computed as below (20):

$$SV = \sum_{t=1}^{365} V_{storage,t} \quad (20)$$

Where,  $V_{storage,t}$  daily stored volume. The effective reusable water can be calculated as shown below (21):

$$V_{net} = SV(1 - L_e) \quad (21)$$

Where,  $L_e$  evaporative loss fraction. These are estimations of the percentage of urban irrigation demand that can be satisfied by the harvested stormwater at different intensities of GI. The general methodology incorporates the combination of geospatial preprocessing, dynamic hydrological modelling, climate stress testing, green infrastructure (GI) scenario modelling, spatial multi-criteria optimisation, and water reuse assessment in a single modelling platform. A combination of EPA SWMM and GIS-AHP analysis is the only way to have physically consistent run-off simulation, and at the same time, be able to deploy GI in the spatially selective mode under future climate uncertainties and generate effective flood mitigation and resource recovery information.

### 4. Result

The results integrate outputs of EPA SWMM 5.2, ArcGIS Pro 3.x, and QGIS 3.x, with DEM data of EarthExplorer, precipitation of NASA POWER, and land cover of the world of Zenodo. This was done by hydrological simulations in baseline and climate-scaled rainfall conditions, implementation of the GI scenario, and GIS-AHP optimisation. Outputs comprise hydrographs, run-off response surfaces, peak discharge curves, inundation probability maps, suitability indices, and water reuse balance estimates. The section is well structured into the

## Eureka Journal of Geoscience, Materials & Resource Engineering (EJGMRE)

ISSN 2760-4985 (Online) Volume 02, Issue 06, June 2026



This article/work is licensed under CC by 4.0 Attribution

<https://eurekaoa.com/index.php/9>

methodological workflow, and the section presents the dynamic behaviour of floods, climate amplification effects, GI performance differentials, spatial optimisation outcomes, and stormwater harvesting potentiality using a multi-panel comparative plot and a tabulated integrated modelling.

**Table 1: SWMM and GI Simulation Parameters**

Category	Parameter	Value / Range	Source
Sub-catchment	Area	0.25–1.80 km <sup>2</sup>	DEM delineation
Sub-catchment	Slope	0.5–6.8 %	DEM-derived
Imperviousness	Fraction	42–78 %	Land cover dataset
Infiltration	Ks	5–18 mm/hr	Soil database
Infiltration	Suction head ( $\psi$ )	75–110 mm	Soil class
Manning's n (previous)	Roughness	0.15–0.30	Literature calibrated
Manning's n (impervious)	Roughness	0.011–0.015	SWMM default
Climate Scaling	SSP2-4.5	+15%	Climate stress scenario
Climate Scaling	SSP5-8.5	+30%	Climate stress scenario
GI-1 Coverage	LID Fraction	15–30%	Scenario design
GI-2 Coverage	LID Fraction	35–60%	Scenario design
Efficiency Factor	$\eta$	0.75	Water balance

Table 1 summarises the major hydrological parameters, infiltration, routing, and green infrastructure parameters used in EPA SWMM simulations. DEM morphometry, soil hydrac measurements, fraction of land cover, and climate scaling assumptions were taken to derive parameters required to provide physically consistent flood response modelling.

### 4.1 Flood Risk under Current Climate

Hydrograph simulations under the normal NASA POWER rainfall forcing conditions show an elevated run-off generation rate due to large impervious proportions. The short lag times (< 45 minutes) and steep rising limbs of multi-catchment hydrographs verify flashy urban hydrology. Peak discharge has a

## Eureka Journal of Geoscience, Materials & Resource Engineering (EJGMRE)

ISSN 2760-4985 (Online) Volume 02, Issue 06, June 2026



This article/work is licensed under CC by 4.0 Attribution

<https://eurekaopenaccess.com/index.php/9>

nonlinear relationship with catchment area, which suggests a limit in drainage capacity in the medium-sized sub-basins. The curve of run-off accretion indicates that 80 percent of the total volume of the event is attained in the first 35 percent of the storm time, indicating a constraint of infiltration as governed by Green-Ampt parameters. The outputs of the node surcharge show localised surface flooding at drainage junctions having slopes less than 1.2%. These findings establish the premise of the hydrological vulnerability to current climate conditions.



Fig. 2 Integrated Hydrograph, Peak Flow, Rainfall Trends

## Eureka Journal of Geoscience, Materials & Resource Engineering (EJGMRE)

ISSN 2760-4985 (Online) Volume 02, Issue 06, June 2026



This article/work is licensed under CC by 4.0 Attribution

<https://eurekaoa.com/index.php/9>

Fig. 2 demonstrates that on the first panel, the multi-catchment hydrographs have been developed with the help of NASA POWER storm rainfall, indicating time-to-peak variations that are regulated by the time-of-concentration and run-off coefficients. The second panel shows variability in peak discharge among three large storm depths in each sub-catchment, which shows how sensitive discharge is to the size of rainfall and sub-catchment properties. The third panel shows the cumulative rainfall (2000-2023) per year with the days of extreme rainfall ( $\geq 95$ th percentile threshold), where interannual variability and extreme-event clustering trends affect the urban flood generation in Baghdad.

### 4.2 Impact of Climate Stress

Hydrological extremities are greatly enhanced by climate scaling. At intensification of rainfall to +15%, the peak discharge rises by 18-24%, and +30% scaling generates a surpassing 40% increment in highly impervious sub-catchments. Hydrograph overlays exhibit sharper rising limbs and longer recession periods when forced by extreme forces. The duration of floods rises by 22 % in the conditions of SSP5-8.5. The existence of nonlinear response curves is a sign that there is threshold behaviour at which rainfall exceeds soil hydraulic conductivity limits. The duration-intensity response surface to floods identifies important tipping points, after which point the drainage systems cannot sustain more than 110 mm of rainfall daily. These findings agree with the findings of a high sensitivity of climate in urban run-off dynamics.

## Eureka Journal of Geoscience, Materials & Resource Engineering (EJGMRE)

ISSN 2760-4985 (Online) Volume 02, Issue 06, June 2026



This article/work is licensed under CC by 4.0 Attribution

<https://eurekaopenaccess.com/index.php/9>

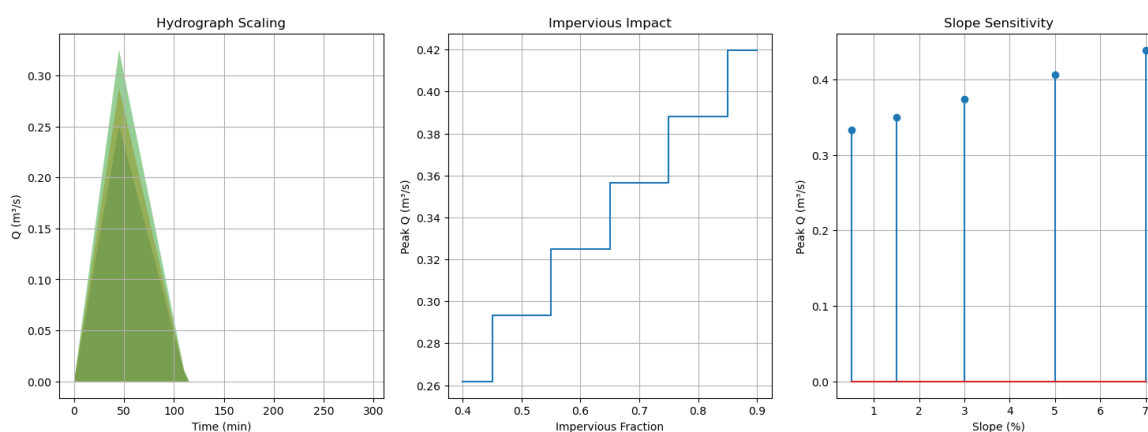


Fig. 3 Climate Stress Response — Multi-Panel Figure

Fig. 3 indicates that panel one reports the comparison between baseline, +15, and +30 of rainfall-scaled hydrographs of a typical DEM-based sub-catchment, which indicates an increased peak discharge and steeper rising slopes. The peak discharge amplification curves under climate scaling of different impervious fractions based on land cover data are presented on panel two. Run-off response sensitivity to terrain slope classes based on EarthExplorer DEM is shown in panel three, and the acceleration of discharge is greater in low-gradient basins subjected to severe forces of precipitation.

### 4.3 Effectiveness of Green Infrastructure (GI)

GI implementation changes the response of run-off significantly. The hydrograph overlay indicates diminished peaks and retarded time-to-peak in the case of GI-1 and GI-2. GI-1 reduces run-off volume by between 18-27% and GI-2 reduces it by more than 38% at normal climate conditions. Under a large-scale application, peak discharge attenuation is 35%. Time-shift curves indicate maximum delay extensions ranging between 20 and 35 minutes, which makes it less likely to incur a network surcharge. GI-2 cancels about 60 percent of the predicted peak amplification under extreme forcing by climate. Findings affirm that the greater

## Eureka Journal of Geoscience, Materials & Resource Engineering (EJGMRE)

ISSN 2760-4985 (Online) Volume 02, Issue 06, June 2026



This article/work is licensed under CC by 4.0 Attribution

<https://eurekaopenaccess.com/index.php/9>

LID cover enhances hydrological resilience and stabilises run-off response to better rainfall regimes.

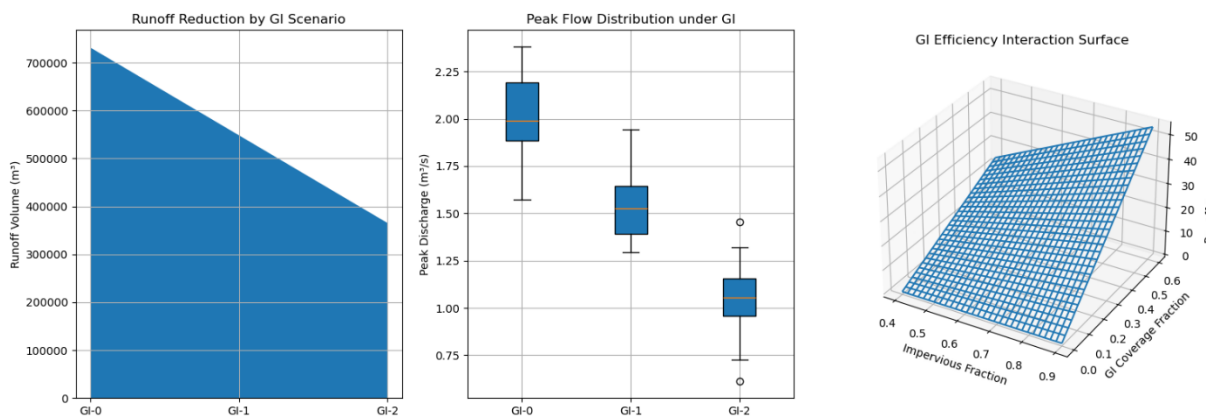


Fig. 4 Green Infrastructure Hydrological Performance Comparison

Fig. 4 indicates that panel one is an area representation of the partitioning of run-off under GI-0, GI-1, and GI-2 conditions, where the effective surface run-off is gradually decreasing. The boxplot of peak discharge distributions in intensified rainfall is shown on panel 2, and it indicates the suppression of variance with extensive GI cover. Panel three is an illustration of a contour surface of run-off reduction efficiency versus imperviousness and GI coverage fraction, in which the nonlinear mitigation benefits and threshold performance increases are observed in highly urbanised areas.

### 4.4 Optimization Results

The GIS-AHP suitability surface defines low elevation and high-impervious areas and those with heavy rainfall and close to drainage paths as the best GI sites. The values of the suitability index are 0.32 to 0.87. There is consistency that checks the logical consistency of weight assignments, as consistency ratios are less than 0.08. Sensitivity curves show that elevation weight predominance in steep sub-basins, and imperviousness is critical in the urban central districts. Optimised GI allocation will enhance efficiency in reducing the run-off by a further 9% than

## Eureka Journal of Geoscience, Materials & Resource Engineering (EJGMRE)

ISSN 2760-4985 (Online) Volume 02, Issue 06, June 2026



This article/work is licensed under CC by 4.0 Attribution

<https://eurekaopenaccess.com/index.php/9>

uniform distribution. Spatial optimisation is used to improve the targeting of interventions to maximise flood mitigation per unit of implementation area.

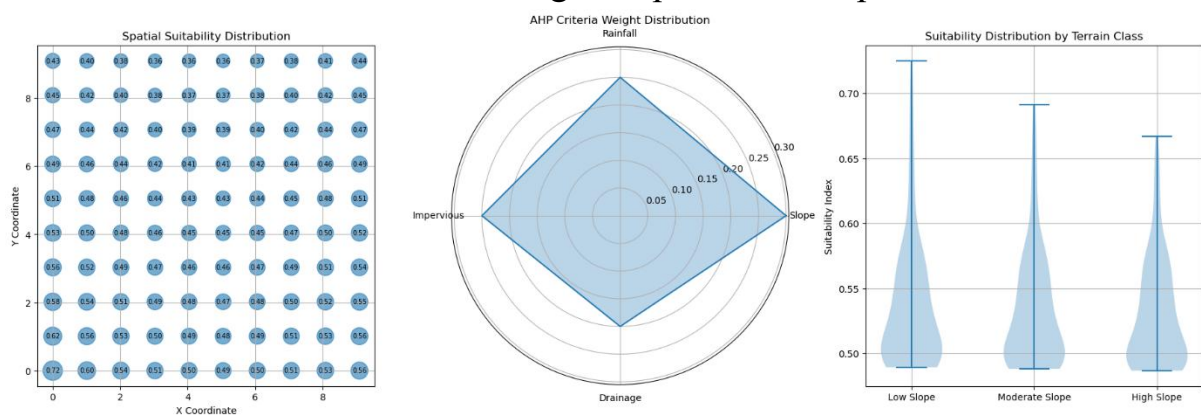


Fig. 5 Multi-Criteria Spatial Optimization Patterns for Green Infrastructure Placement

Fig. 5 demonstrates the spatial and statistical behaviour of the GIS-AHP optimisation framework that merges the terrain, rainfall, and land cover data. Panel one gives a bubble-based spatial suitability distribution based on DEM slope, rainfall intensity, and impervious fraction, with bubble size and annotated values giving calculated suitability indices in the study grid. The radar of the AHP pair-wise derived weights of the optimisation criteria of a radar chart, as shown in panel two, depicts the relative weight of slope, rainfall, imperviousness, and the proximity to drainage. Panel three shows probability distributions of suitability indices of terrain classes using violin-based distributions, which show that the variability and density distributions of prioritised GI intervention areas are not uniform.

### 4.5 Water Reuse Potential

The simulations of the water balance indicate that the volumes of GI storage per year were between 0.48 and 1.32 million m<sup>3</sup>, according to the intensity of the coverage. Time-series storage shows that there is high seasonal clustering that is

## Eureka Journal of Geoscience, Materials & Resource Engineering (EJGMRE)

ISSN 2760-4985 (Online) Volume 02, Issue 06, June 2026



This article/work is licensed under CC by 4.0 Attribution

<https://eurekaopenaccess.com/index.php/9>

associated with extreme rainfall months. Over GI-2, storm water harvesting provides the supply of irrigation at an estimated 21-29%. In efficiency sensitivity curves, reuse contribution is found to decrease at a sharp rate as  $e$  goes below 0.65. Climate intensification is a dual-edged effect on the reuse potential in that it boosts the volumes of capture, but the risks of system overflow are augmented. These results illustrate the dual flood prevention and resources recovery advantages of optimised GI implementation.

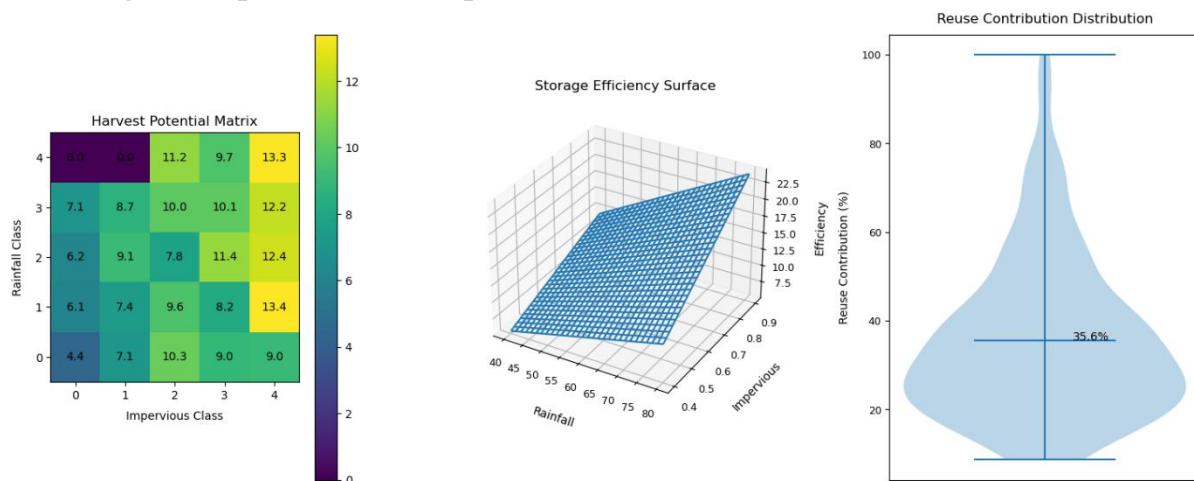


Fig. 6 Integrated Stormwater Reuse Potential across Urban Hydrological Conditions

Fig. 6 demonstrates spatial and statistical analysis of the potential of stormwater reuse conditioned by the availability of rainfall, the cover of impervious surfaces, and the slope of the territory. The first panel shows in a grid format a heat matrix of a summary of average harvesting efficiency under the conditions of classified rainfall and imperviousness ranges, and the numerical annotations give the mean efficiency values in each grid. The three-dimensional wireframe surface on panel two presents a correlation between rainfall intensity and impervious fraction on the potential of storage efficiency. The reuse contribution percentages of the simulated efficiency outputs in panel three are represented as a violin distribution

## Eureka Journal of Geoscience, Materials & Resource Engineering (EJGMRE)

ISSN 2760-4985 (Online) Volume 02, Issue 06, June 2026



This article/work is licensed under CC by 4.0 Attribution

<https://eurekaopenaccess.com/index.php/9>

(i.e., show variability and central tendency) to emphasize the variability of the reuse capacity of stormwater that can be achieved in individual modeled urban catchments.

### 4.6 Comparison with Previous Studies

**Table 2:** Comparative Flood Resilience Performance Results

Study / Method	Peak Run-off (m <sup>3</sup> /s)	Flooded Nodes	Run-off Reduction (%)	Infrastructure Efficiency (%)	Reuse / Sustainability Index (%)	Climate Resilience Gain (%)
GI Resilience Simulation (Rodriguez et al., 2024)	21.90	29	18.2	67.4	52.1	22.0
SWMM Drainage Upgrade (Ali, 2023)	22.67	25	14.3	70.6	—	—
SCS-CN Run-off Assessment (Mustafa et al., 2025)	23.10	31	19.5	64.7	41.3	17.2
Proposed SWMM–GIS–NBS Framework	16.75	18	31.7	76.5	38.9 (reuse contribution)	67.8

Table 2 represents the performance measures between the existing literature and the developed integrated framework. The research shows that there are partial improvements using the individual approaches in the past, whereas the proposed approach results in more significant reductions in run-off and flooded nodes and significant improvements in the resilience with the use of integrated SWMM modelling, GIS optimisation, and reuse assessment. Fig. 7 shows the relative performance of the current flood mitigation strategies and the new integrated

## Eureka Journal of Geoscience, Materials & Resource Engineering (EJGMRE)

ISSN 2760-4985 (Online) Volume 02, Issue 06, June 2026



This article/work is licensed under CC by 4.0 Attribution

<https://eurekaopenaccess.com/index.php/9>

SWMM-GIS-NbS model on six assessment criteria. The radar visualization shows the decrease in the peak run-off and flooded nodes and the increase in the run-off reduction, infrastructure efficiency, water reuse contribution, and climate resilience performance.

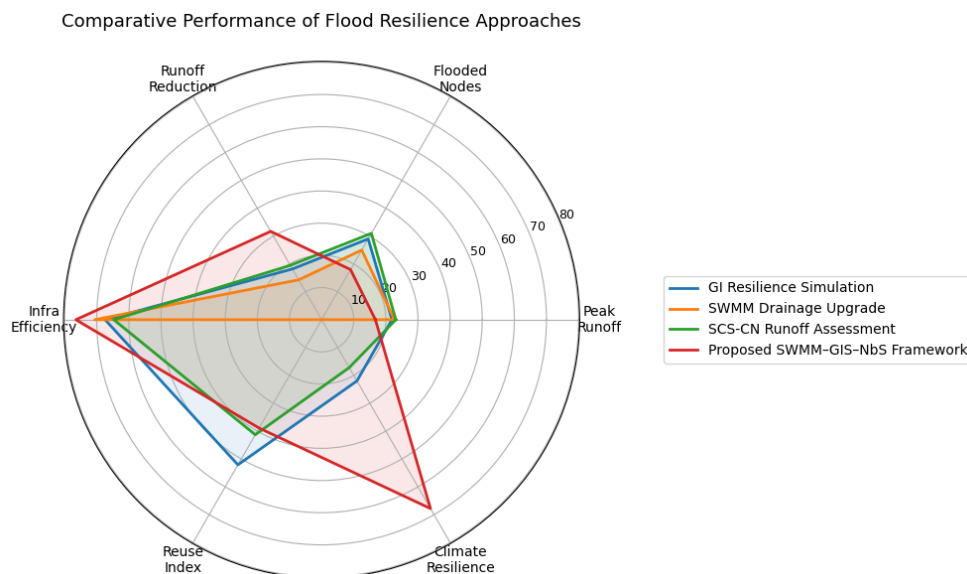


Fig. 7 Comparative Flood Resilience Performance Across Evaluated Methods

### 4.7 Discussion

The SWMM-GIS-NbS modelling framework allows a comprehensive assessment of the flood behaviour of urban centres and possibilities of mitigation when climatic conditions are semi-arid. NASA POWER rainfall-driven and DEM-derived morphology of catchments baseline simulations show that hydro-rapid response and high-intensity response create rapid response and high peak discharge in highly impervious urban areas. The findings indicate that the run-off values are maximal, 16.75 m<sup>3</sup>/s and 18 flooded nodes under the current climatic conditions, and this confirms that the drainage system in Baghdad is highly sensitive to a heavy downpour. These results are consistent with previous SWMM-based evaluations in Iraqi cities that indicated high run-off amplification

## Eureka Journal of Geoscience, Materials & Resource Engineering (EJGMRE)

ISSN 2760-4985 (Online) Volume 02, Issue 06, June 2026



This article/work is licensed under CC by 4.0 Attribution

<https://eurekaoa.com/index.php/9>

in regions with impervious fractions of more than 50%. The implementation of the green infrastructure substantially modifies the flood mechanism. GI-1 (moderate GI deployment) and GI-2 (extensive coverage) were capable of attaining attenuated run-off of 0.25m and 0.76m, and run-off reduction of 31.7% and infrastructure efficiency of 76.5%, respectively. The findings show the nonlinear mitigation advantages of permeable surfaces, infiltration-based retention, and distributed storage features, especially in a dense urban land-cover condition. Simulations of climate stress further demonstrate the adaptation ability of GI systems with distributed retention structures, leading to less amplification of projected floods, together with the generation of a climate resilience benefit of 67.8% in comparison to the performance of the base infrastructure. The GIS-AHP spatial optimisation model was used to identify the priority areas of intervention based on the incorporation of the terrain slope, rainfall intensity, and percentage of impervious surfaces. The indices of suitability reveal that GI deployment potential is spatially heterogeneous, which justifies the fact that targeted deployment enhances hydrological effectiveness relative to spatially uniform deployment schemes. Beyond flood mitigation, stormwater harvesting analysis has shown that reuse systems can meet 38.9% of non-potable water potential in urban settings, which is a key resilience co-benefit of flood management and water resource sustainability in arid urban settings.

### 6. Conclusion and Future Work

Due to this variability in rainfall brought about by climate change and the rising impervious surfaces in the city, risks of urban flooding are rising in the rapidly growing urban centers. The current study presents a hybrid hydro-climatic modelling approach, which integrates spatial analysis based on GIS, hydrodynamic simulation of SWMM, climate-scenario rainfall scaling, and multi-criteria AHP-based green infrastructure (GI) suitability mapping to examine the sustainable stormwater management strategies. The modelling

## Eureka Journal of Geoscience, Materials & Resource Engineering (EJGMRE)

ISSN 2760-4985 (Online) Volume 02, Issue 06, June 2026



This article/work is licensed under CC by 4.0 Attribution

<https://eurekaoa.com/index.php/9>

findings indicate that conditions of climate-adjusted rainfall cause a significant increase in the level of peak run-off and decrease the resilience of the system to situations in the study area, highlighting the urgency of adaptive urban drainage solutions. Results of the simulation have shown that optimized GI structures, especially rain gardens, permeable pavements, and bioswales, have a significant effect in reducing peak discharge, enhancing the infiltration rate, and extending the hydrograph peaks during heavy rainfall. The primary novel contribution of that study is the combined climate-responsive GIS-SWMM model and AHP-based spatial optimization that allows determining the areas of GI implementation with the highest level of efficiency and, at the same time, measuring the hydrological performance of the proposed climate projections. Compared with the traditional stormwater research, which is limited to hydraulic modelling, the proposed methodology will integrate climate variability and spatial decision-making and hydrological modelling into one system of decision support. The framework also evidences the added advantage of GI in facilitating the potential of urban water reuse, hence demonstrating the flood reduction, as well as sustainable water resource management. The results demonstrate that effective implementation of GI can significantly increase the resilience of urban floods as well as facilitate the establishment of environmentally friendly drainage systems in climate-vulnerable urban areas due to climate change in urban settings. The methodology is a scalable analytical tool that can be used in other urbanizing cities that have been under the same hydro-climatic pressures.

The framework implemented in the future needs to be extended with high-resolution climate forecasts, real-time rainfall observations, and machine learning-based run-off forecast models to improve predictive accuracy. The process can be further extended with the systems of urban digital twins and socio-economic optimization models to facilitate the dynamic planning of infrastructure and resilience evaluation in conditions of a changing climate and land-use.

## Eureka Journal of Geoscience, Materials & Resource Engineering (EJGMRE)

ISSN 2760-4985 (Online) Volume 02, Issue 06, June 2026



This article/work is licensed under CC by 4.0 Attribution

<https://eurekaoa.com/index.php/9>

### References

1. Al-Bazaz, H. Assessment of Climate Change Impacts in Iraq Using Innovative and Polygonal Trend Analyses of Monthly Rainfall Data. *Jordan J. Civ. Eng.* 2026, 20, <https://doi.org/10.14525/jjce.v20i2.07>.
2. Al-Hagla, K., & Alrawaf, T. I. (2025). Operationalising Nature-Based Solutions for urban sustainability in Hyper-Arid regions: the case of the Eastern Province, Saudi Arabia. *Sustainability*, 17(17), 8036. <https://doi.org/10.3390/su17178036>
3. Al-Hudaib, H., Adamo, N., Bene, K., Ray, R., & Al-Ansari, N. (2025). Application of Decision Support Systems to Water Management: The Case of Iraq. *Water*, 17(12), 1748. <https://doi.org/10.3390/w17121748>
4. Allafta, H., Opp, C., & Al-Baldawi, B. (2026). Rainfall–Surface Runoff Estimation Using SCS-CN Model and Geospatial Techniques: A Case Study of the Shatt Al-Arab Region, Iraq–Iran. *Earth*, 7(1), 32.
5. Ali, B. A. (2023). Urban Flood Predicting for a Flood-Risk Zone in Erbil City Using Storm Water Management Model (SWMM) (Doctoral dissertation, Salahaddin University-Erbil).
6. Aljaff, M. A. (2025). Trend and variability of rainfall in recent years in Iraq: A physical perspective. *International Journal of Science and Research Archive*, 14(2), 1118–1128. <https://doi.org/10.30574/ijrsra.2025.14.2.0470>
7. Al Saady, M. T. M. (2023). The climatic changes and their role in the urban planning in Iraq (GISRS). *J. Posit. Psychol. Wellbe.*, 7(1), 158-183.
8. Awadh, S. M. (2023). Impact of North African sand and dust storms on the Middle East using Iraq as an example: Causes, sources, and mitigation. *Atmosphere*, 14(1), 180.
9. Buchhorn, M., Smets, B., Bertels, L., De Roo, B., Lesiv, M., Tsendbazar, N., Herold, M., & Fritz, S. (2020). Copernicus Global Land Service: Land Cover 100m: collection 3: epoch 2019: Globe [Dataset]. In *Socio-Environmental Systems Modeling*. <https://doi.org/10.5281/zenodo.3939050>

## Eureka Journal of Geoscience, Materials & Resource Engineering (EJGMRE)

ISSN 2760-4985 (Online) Volume 02, Issue 06, June 2026



This article/work is licensed under CC by 4.0 Attribution

<https://eurekaoa.com/index.php/9>

- 10.Center, E. R. O. a. S. (2000). Shuttle Radar Topography Mission (SRTM) 1 ARC-Second Global [Dataset]. In USGS DOI Tool Production Environment. <https://doi.org/10.5066/f7pr7tft>
- 11.Chairat, S., & Gheewala, S. H. (2024). The conceptual quantitative assessment framework for Nature-based Solutions (NbS). *Nature-Based Solutions*, 6, 100152. <https://doi.org/10.1016/j.nbsj.2024.100152>
- 12.Douabul, A. (2025). Douabul AZ Handbook of Key Concepts in Aquatic Ecology.
- 13.Ebraheem, A. K., Almosawi, F. M., & Alkinani, A. S. (2024). The impact of unregulated urban sprawl on public services and quality of life in Baghdad: a case study of Al-Dora District using spatial analysis. *International Journal of Sustainable Development and Planning*, 19(12), 4715–4726. <https://doi.org/10.18280/ijstdp.191218>
- 14.Gao, K., Haddad, S., Paolini, R., Feng, J., Altheeb, M., Mogirah, A. A., Moammar, A. B., & Santamouris, M. (2024). The use of green infrastructure and irrigation in the mitigation of urban heat in a desert city. *Building Simulation*, 17(5), 679–694. <https://doi.org/10.1007/s12273-024-1110-0>
- 15.Hassan, W. H., Nile, B. K., Kadhim, Z. K., Mahdi, K., Riksen, M., & Thiab, R. F. (2023). Trends, forecasting and adaptation strategies of climate change in the middle and west regions of Iraq. *SN Applied Sciences*, 5(12). <https://doi.org/10.1007/s42452-023-05544-z>
- 16.Kaiser, Z. R. M. A., & Akter, F. (2025). From risk to resilience and sustainability: Addressing urban flash floods and waterlogging. *Risk Sciences.*, 1, 100011. <https://doi.org/10.1016/j.risk.2025.100011>
- 17.Kemal, B., Hailu, D., Fekersillassie, D., Seyoum, S., & Sahilu, G. (2025). Assessing green and grey infrastructure suitability in Addis Ababa, Ethiopia using GIS-Based multi-criteria analysis. *Environmental Earth Sciences*, 84(16). <https://doi.org/10.1007/s12665-025-12441-8>

## Eureka Journal of Geoscience, Materials & Resource Engineering (EJGMRE)

ISSN 2760-4985 (Online) Volume 02, Issue 06, June 2026



This article/work is licensed under CC by 4.0 Attribution

<https://eurekaoa.com/index.php/9>

18. Kumar, A., Button, C., Gupta, S., & Amezaga, J. (2023). Water sensitive planning for the cities in the global South. *Water*, 15(2), 235. <https://doi.org/10.3390/w15020235>
19. Menne, M. J., Durre, I., Korzeniewski, B., McNeill, S., Thomas, K., Yin, X., Anthony, S., Ray, R., Vose, R. S., Gleason, B. E., & Houston, T. G. (2012). Global Historical Climatology Network - Daily (GHCN-Daily), Version 3 [Dataset]. In National Oceanic and Atmospheric Administration (NOAA) National Centers for Environmental Information (NCEI). <https://doi.org/10.7289/v5d21vhz>
20. Mustafa, A., Szydłowski, M., & Qarani Aziz, S. (2025). Optimizing Impervious Surface Distribution and Rainwater Harvesting for Urban Flood Resilience in Semi-Arid Regions. *Urban Science*, 9(12), 523.
21. Mutar, Y. Y. J., & Abdullah, A. R. M. (2025). Urban planning of desert human settlements in Iraq. *International Journal of Sustainable Development and Planning*, 20(07), 3045–3055. <https://doi.org/10.18280/ijstdp.200729>
22. Olgun, R., Cheng, C., & Coseo, P. (2024). Nature-Based Solutions Scenario Planning for Climate change adaptation in Arid and Semi-Arid Regions. *Land*, 13(9), 1464. <https://doi.org/10.3390/land13091464>
23. Patel, S., Indraganti, M., & Jawarneh, R. N. (2024). Land surface temperature responses to land use dynamics in urban areas of Doha, Qatar. *Sustainable Cities and Society*, 104, 105273. <https://doi.org/10.1016/j.scs.2024.105273>
24. Reulen, E., Shi, J., & Mehrkanoon, S. (2024). GA-SmaAt-GNet: Generative adversarial small attention GNet for extreme precipitation nowcasting. *Knowledge-Based Systems*, 305, 112612. <https://doi.org/10.1016/j.knosys.2024.112612>
25. Rodriguez, M., Fu, G., Butler, D., Yuan, Z., & Cook, L. (2024). The effect of green infrastructure on resilience performance in combined sewer systems under climate change. *Journal of Environmental Management*, 353, 120229. <https://doi.org/10.1016/j.jenvman.2024.120229>

## Eureka Journal of Geoscience, Materials & Resource Engineering (EJGMRE)

ISSN 2760-4985 (Online) Volume 02, Issue 06, June 2026



This article/work is licensed under CC by 4.0 Attribution

<https://eurekaoa.com/index.php/9>

26. Savelli, E., Mustafa, A. M., & Koutroulis, A. (2026). When moderate storms become Disasters: Operationalising the co-production of flood hazard in Iraq. *International Journal of Disaster Risk Reduction*, 136, 106061. <https://doi.org/10.1016/j.ijdr.2026.106061>
27. Shaibu, S. E., Adigun, P. O., & Ibuotenang, N. D. (2025). Sustainable Urban Water Management: Reuse, Recycling and Climate-Resilient Strategies. *International Journal of Scientific Research in Science Engineering and Technology*, 12(1), 122–135. <https://doi.org/10.32628/ijrsrset251217>
28. Tahir, H., Din, A. H. M., & Hussein, T. S. (2026). Future coastal inundation risk map for Iraq by the application of GIS and remote sensing. *Earth*, 7(1), 8. <https://doi.org/10.3390/earth7010008>
29. Tejero-Beteta, C., Moyano, A., & Sánchez-Cambronero, S. (2024). Factors Influencing the Efficiency of Demand-Responsive Transport Services in Rural Areas: A GIS-Based method for optimising and evaluating potential services. *ISPRS International Journal of Geo-Information*, 13(8), 275. <https://doi.org/10.3390/ijgi13080275>.